Electronic Supplementary Material (ESI) for ChemComm.

Electronic Supplementary Information

Kota Oishi, Koki Muraoka*, Akira Nakayama*

Department of Chemical System Engineering, The University of Tokyo, 7-3-1 Hongo, Bunkyo-ku, Tokyo 113-8656 (Japan)

*E-mail: nakayama@chemsys.t.u-tokyo.ac.jp

Methods

This study employed the Preferred Potential (PFP)[1] version 4.0.0 as the universal neural network potential for structure optimization. D3 dispersion correction[2] was applied to PFP to account for long-range interaction. A combined optimization using FIRE[3] and LBFGS[4] was used to relax zeolite–OSDA complexes until the minimum force was less than 0.01 eV/Å. In the vibrational frequency calculations, the displacement of each atom from the equilibrium structure was set to 0.015 Å. A code snippet to reproduce our simulation data is provided in the Supplementary Note. Plane-wave, periodic DFT calculations using PBE functionals were performed to compute single-point energies for optimized structures with the Vienna Ab initio Simulation Package (VASP),[5] version 5.4.4. The calculation condition was MPStatic implemented in pymatgen version 2023.3.23[6] with D3 dispersion correction.[2, 7] The initial structures of FER–OSDA complexes were created from XRD-derived structures,[8] which is a 1 × 1 × 2 supercell. We first removed all OSDAs and relaxed the silica frameworks using PFP. Then, one OSDA was introduced to the cell containing 72 Si sites. Subsequently, one Si site was replaced with Al. The workflow as mentioned earlier was applied to the 72 structures.

CHA–OSDA complexes were obtained from the OSDB database (last accessed January, 2023).[9] The structures were expanded to 2 × 2 × 2 supercells. After removal of OSDAs, the silica frameworks were optimized. Then one OSDA was added back to the supercell. Subsequently, one Si site in the CHA cage with an OSDA inside was replaced with Al.

The general linear models were constructed using R statistical software. Gamma regression was performed, assuming a gamma distribution of relative energies, with the inverse function serving as the link function.

We employed the Sanders–Leslie–Catlow (SLC) potential[10] as implemented in the General Utility Lattice Program (GULP)[11] to calculate lattice parameters and geometric descriptors for silica FER and CHA to validate PFP. It was also used to calculate defect energies with the Mott–Littleton methodology[12]. The size of region I was 20 Å (i.e., 3044 ions) and that of region IIa was 26 Å. Bader charge partitioning[13] was used to evaluate charge distributions of stable FER–OSDA complexes obtained by DFT.

Supplementary Note

Code snippet to reproduce our calculation setting using PFP.

```
from matlantis_features.ase_ext.optimize import FIRELBFGS
from pfp_api_client.pfp.calculators.ase_calculator import ASECalculator
from pfp_api_client.pfp.estimator import EstimatorCalcMode, Estimator

from pymatgen.io.ase import AseAtomsAdaptor
from ase.constraints import UnitCellFilter
from ase.phonons import Phonons
from ase.thermochemistry import CrystalThermo

estimator = Estimator()
estimator.set_calc_mode(EstimatorCalcMode.CRYSTAL_PLUS_D3)
calculator = ASECalculator(estimator)
atoms.calc = calculator
ucf = UnitCellFilter(atoms)
dyn = optimizer(ucf)
dyn.run(fmax=fmax)
e = atoms.get_potential_energy()

ph = Phonons(atoms, calculator, supercell=(1,1,1), delta=0.015)
ph.run()
ph.read(acoustic=True)
phonon_energies, phonon_DOS = ph.dos(kpts=(10, 10, 10), npts=1000, elta=1e-3)
thermo = CrystalThermo(
   phonon_energies=phonon_energies,
   phonon_DOS=phonon_DOS,
   potentialenergy=e,
)
F = thermo.get_helmholtz_energy(temperature=300)
```

Supplementary Figures

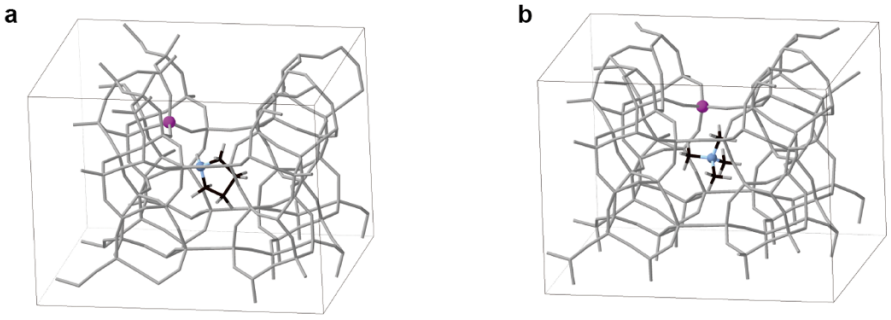

Fig. S1 Most stable structures of (a) PYRR–FER and (b) TMA–FER.

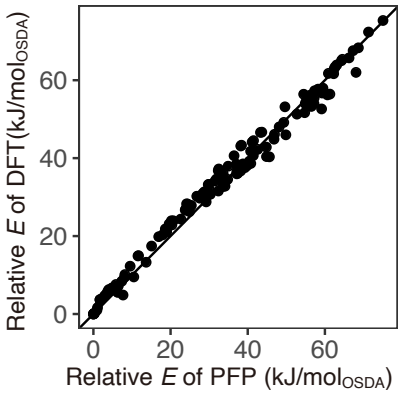

Fig. S2 Relationship between relative energies calculated by PFP and those by DFT for FER with TMA and PYRR.

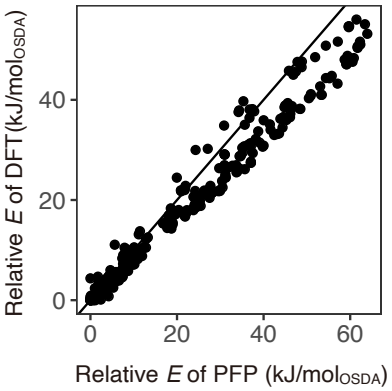

Fig. S3 Relationship between relative energies calculated by PFP and those by DFT for CHA with TMA, TEA, TriEA, TMAda, DMAda, P1AD, and P2AD.

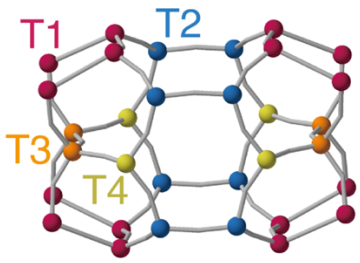

Fig. S4 The crystal structure of FER-type zeolite with crystallographically different tetrahedral (T) sites (spheres). Cylinders are T–O bonds.

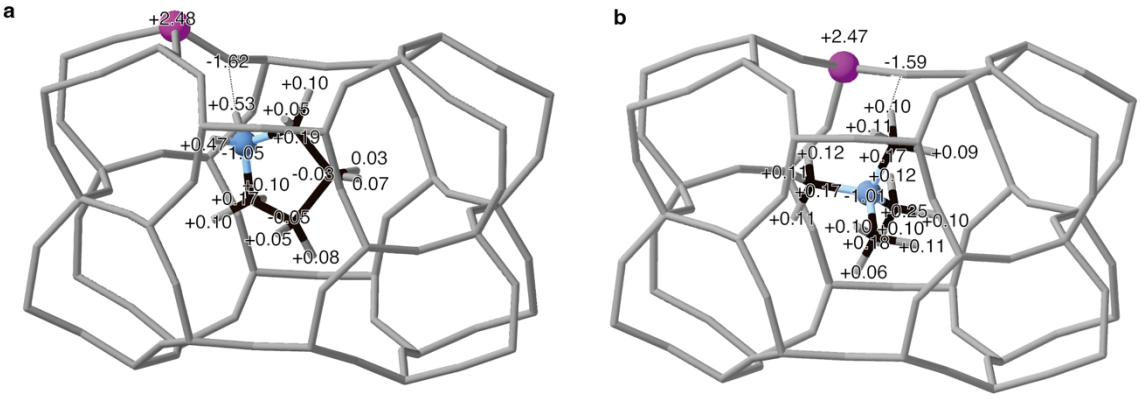

Fig. S5 Charge distribution of (a) PYRR–FER and (b) TMA–FER determined by the Bader charge analysis.

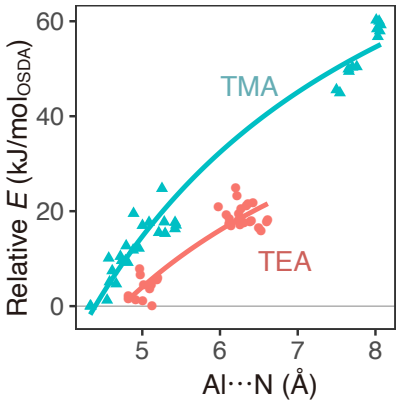

Fig. S6 The relationship between relative energy and Al···N distance of TMA–CHA and TEA–CHA.

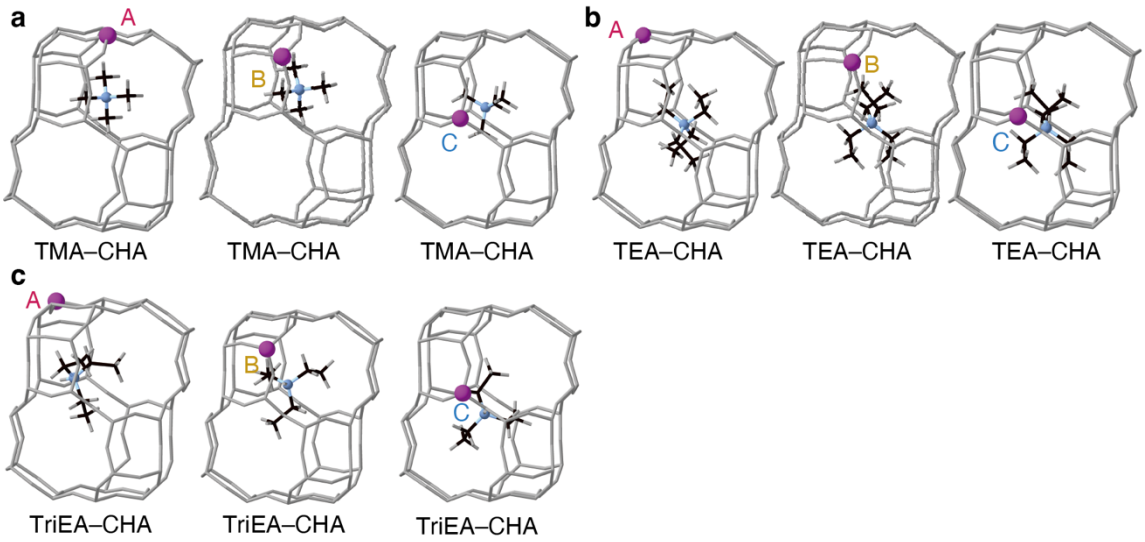

Fig. S7 Stable zeolite–OSDA complexes for (a) TMA–CHA, (b) TEA–CHA, and (c) TriEA–CHA for each Al distribution.

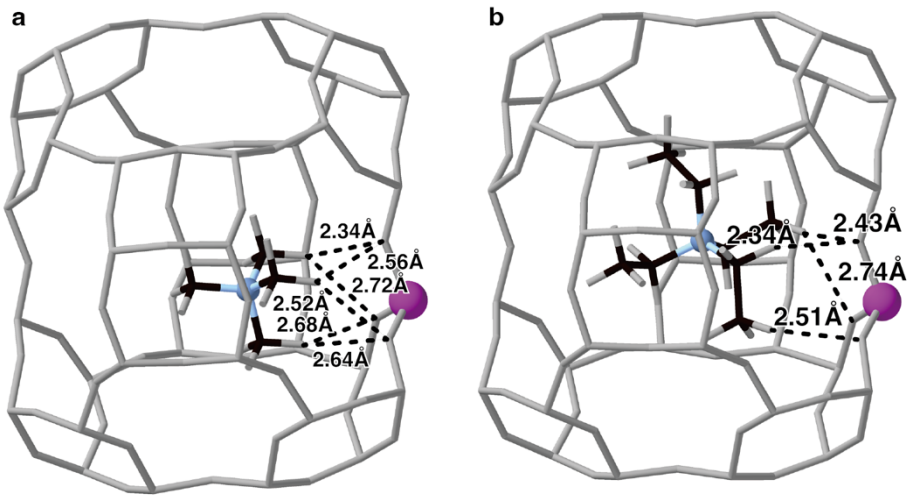

Fig. S8 Stable zeolite–OSDA complexes and the distance between H(–N) and O(–Al) for (a) TMA–CHA, and (b) TEA–CHA.

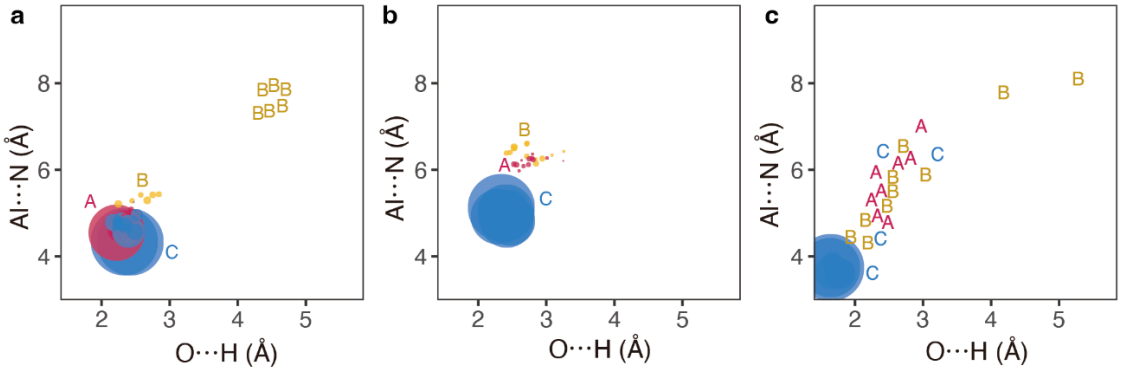

Fig. S9 Relationship between O···H distance, Al···N distance and probability of (a) TMA–CHA, (b) TEA–CHA, and (c) TriEA–CHA.

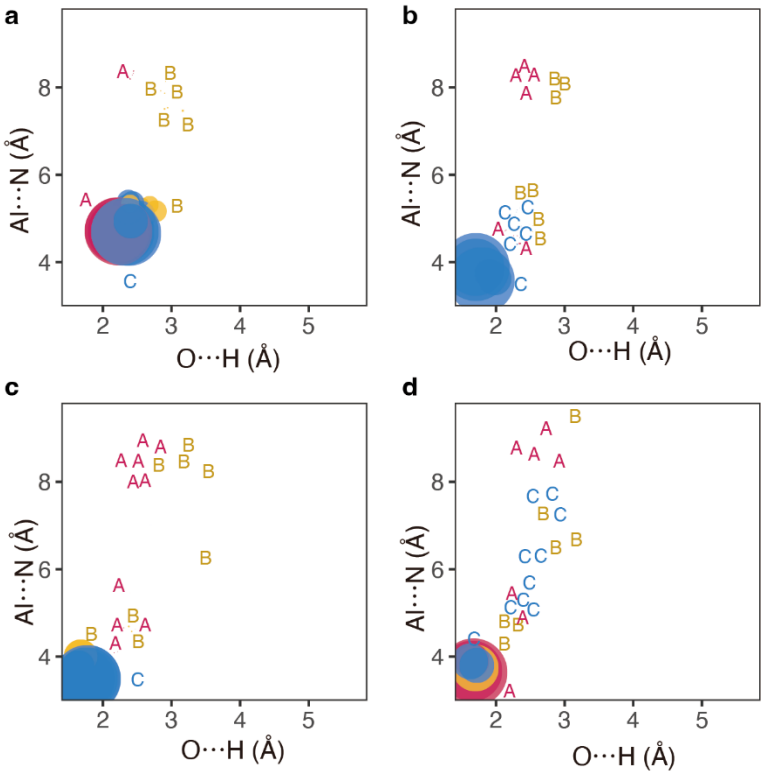

Fig. S10 (a–d) Relationship between O···H distance, Al···N distance and probability of (a) TMAda–CHA, (b) DMAda–CHA, (c) P1AD–CHA, and (d) P2AD–CHA.

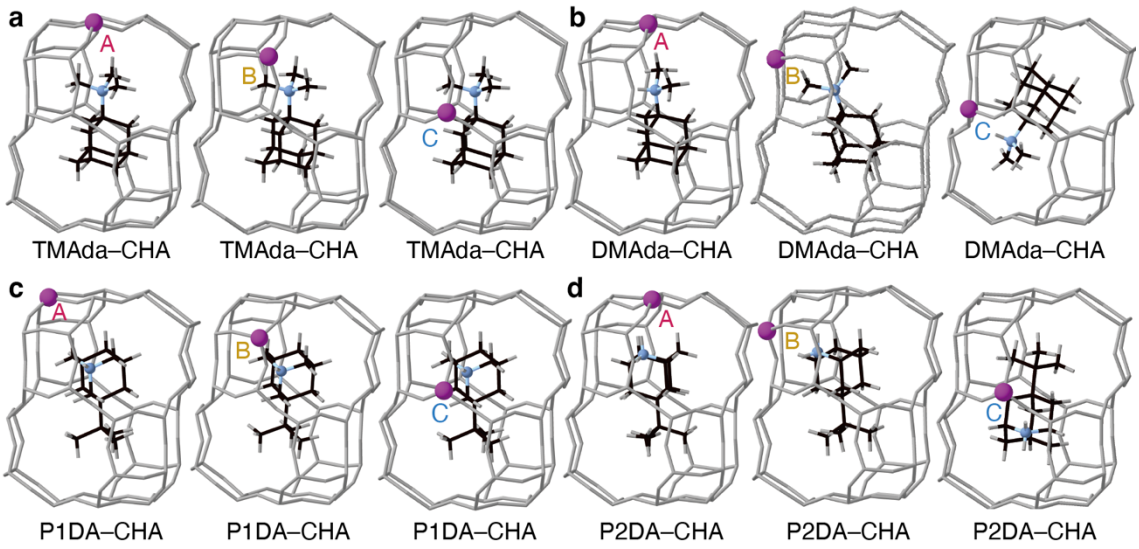

Fig. S11 Stable zeolite–OSDA complexes for (a) TMAda–CHA, (b) DMAda–CHA, (c) P1AD–CHA, and (d) P2AD–CHA for each Al distribution. Purple spheres represent Al, grey rods indicate the silicate framework, light blue spheres represent N, and black and white rods signify C and H, respectively.

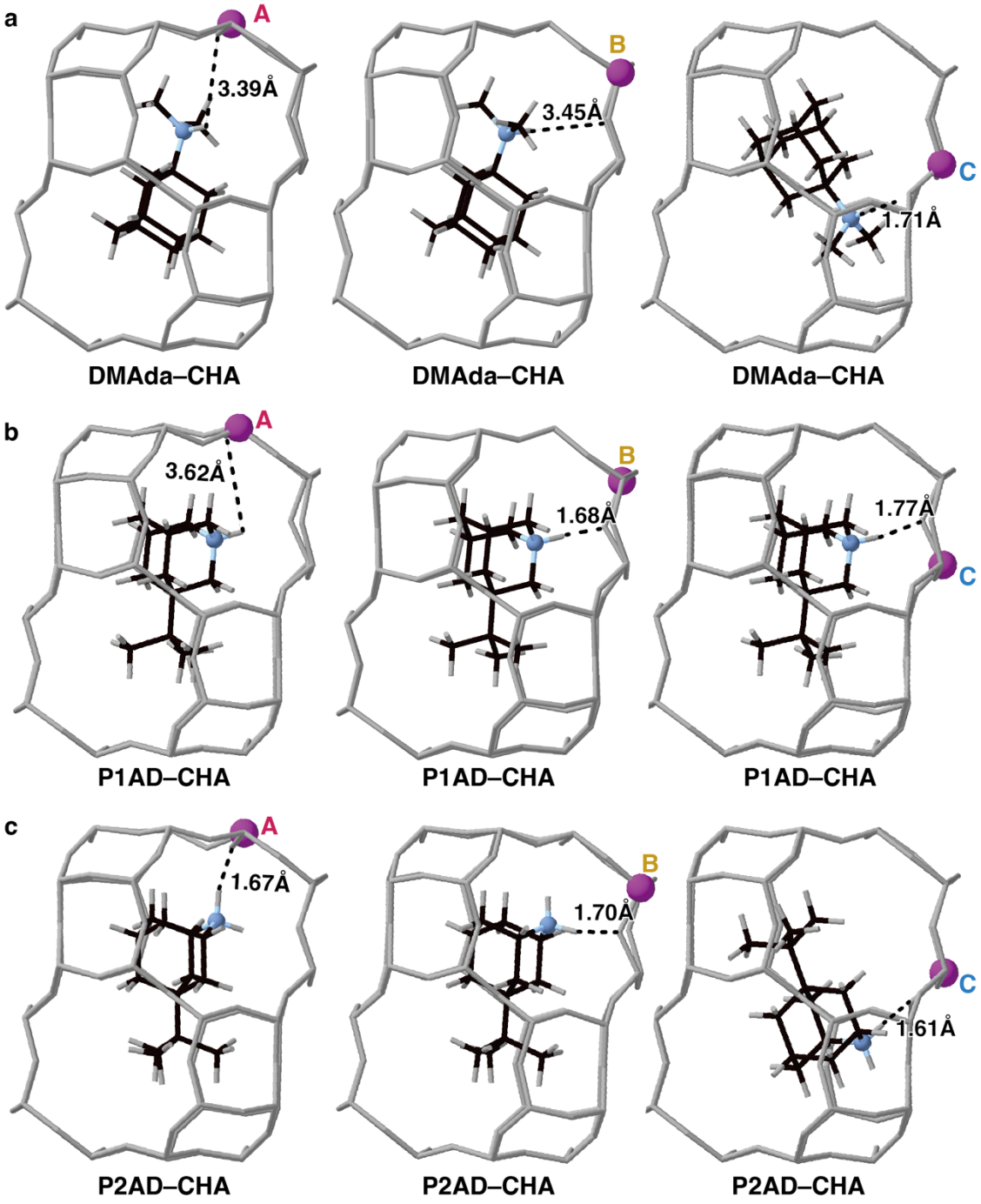

Fig. S12 Zeolite–OSDA complexes and the distance between H(–N) and O(–Al) for (a) DMAda–CHA, (b) P1AD–CHA, and (c) P2AD–CHA.

Supplementary Tables

Table S1 Energy (kJ/mol) of the most energetically favoured configurations for each site with respect to that of T1 site for FER-PYRR complex.

T site for Al	Energy					Free energy (300 K)
	PBE+D3	PBEsol	SCAN	BEEF-vdW	PFP+D3	PFP+D3
T1	0.000	1.831	0.608	0.102	0.000	0.000
T2	1.669	0.000	0.000	0.000	1.079	2.393
T3	14.923	11.253	17.095	13.736	11.561	15.736
T4	6.740	3.092	4.858	7.079	5.147	8.054

Table S2 Defect energies for FER.

T site for Al	Defect energy (eV)	Relative energy (kJ/mol)
T1	38.1582	0.00
T2	38.1805	2.14
T3	38.1667	0.82
T4	38.1810	2.20

Table S3 Relative energy for FER-TMA with respect to the energy of T2 site.

T site for Al	Relative energy (kJ/mol)				
	PFP	PBE	PBEsol	SCAN	BEEF
T1	1.803	3.471	4.692	3.465	2.027
T2	0.000	0.000	0.000	0.000	0.000
T3	9.528	12.291	12.475	12.647	10.952
T4	5.842	7.601	2.659	2.875	0.840

Table S4 Crystallographic parameters for pure silica FER. The values represent min–max [average].

	Experimental data[14]	PFP	Forcefield (SLC)
∠(Si–O–Si) (°)	143.7–174.8 [155.1]	147.9–179.7 [156.0]	150.1–180.0 [156.0]
d(Si–O) (Å)	1.580−1.602 [1.593]	1.606–1.624 [1.619]	1.608–1.610 [1.609]
d(Si–Si) (Å)	Not Available	3.115−3.240 [3.156]	3.110–3.122 [3.147]
a (Å)	18.820	19.111	18.808
b (Å)	14.092	14.291	15.053
c (Å)	7.430	7.556	7.444
α (°)	90	90.000	90.000
β (°)	90	90.000	90.000
γ (°)	90	90.000	90.000

Table S5 Crystallographic parameters for pure silica CHA. The values represent min–max [average].

	Experimental data[15]	PFP	Forcefield (SLC)
∠(Si–O–Si) (°)	[148.4]	146.1–150.1 [147.6]	147.8–150.1 [149.2]
d(Si–O) (Å)	[1.603]	1.618–1.630 [1.623]	1.608–1.611 [1.610]
d(Si–Si) (Å)	Not Available	3.101–3.241 [3.118]	3.091–3.112 [3.103]
a (Å)	13.529	13.751	13.536
b (Å)	13.529	13.751	13.536
c (Å)	14.748	14.727	14.553
α (°)	90	90.000	90.000
β (°)	90	90.000	90.000
γ (°)	120	120.000	120.000

1 S. Takamoto, C. Shinagawa, D. Motoki, K. Nakago, W. Li, I. Kurata, T. Watanabe, Y. Yayama, H. Iriguchi, Y. Asano, T. Onodera, T. Ishii, T. Kudo, H. Ono, R. Sawada, R. Ishitani, M. Ong, T. Yamaguchi, T. Kataoka, A. Hayashi, N. Charoenphakdee and T. Ibuka, *Nat. Commun.*, 2022, **13**, 1–11.
2 S. Grimme, J. Antony, S. Ehrlich and H. Krieg, *J. Chem. Phys.*, 2010, **132**, 154104.
3 E. Bitzek, P. Koskinen, F. Gähler, M. Moseler and P. Gumbsch, *Phys. Rev. Lett.*, 2006, **97**, 170201.
4 D. C. Liu and J. Nocedal, *Math Program*, 1989, **45**, 503–528.
5 G. Kresse and J. Furthmüller, *Phys. Rev. B*, 1996, **54**, 11169.
6 A. Jain, S. P. Ong, G. Hautier, W. Chen, W. D. Richards, S. Dacek, S. Cholia, D. Gunter, D. Skinner, G. Ceder and K. A. Persson, *APL Mater.*, 2013, **1**, 011002.
7 S. Grimme, S. Ehrlich and L. Goerigk, *J. Comput. Chem.*, 2011, **32**, 1456–1465.
8 A. B. Pinar, L. Gómez-Hortigüela, L. B. McCusker and J. Pérez-Pariente, *Chem. Mater.*, 2013, **25**, 3654–3661.
9 D. Schwalbe-Koda, S. Kwon, C. Paris, E. Bello-Jurado, Z. Jensen, E. Olivetti, T. Willhammar, A. Corma, Y. Román-Leshkov, M. Moliner and R. Gómez-Bombarelli, *Science*, 2021, **374**, 308–315.
10 M. J. Sanders, M. Leslie and C. R. A. Catlow, *J. Chem. Soc. Chem. Commun.*, 1984, **19**, 1271–1273.
11 J. D. Gale, *J. Chem. Soc., Faraday Trans.*, 1997, **93**, 629–637.
12 N. F. Mott and M. J. Littleton, *Trans. Faraday Soc.*, 1938, **34**, 485–499.
13 W. Tang, E. Sanville and G. Henkelman, *J. Phys. Condens. Matter*, 2009, **21**, 84204–84211.
14 J. E. Lewis, C. C. Freyhardt and M. E. Davis, *J. Phys. Chem.*, 1996, **100**, 5039–5049.
15 M. J. Díaz-Cabañas, P. A. Barrett and M. A. Camblor, *Chem. Commun.*, 1998,**17**, 1881–1882.